Molecular Dynamics Study on Class A β-Lactamase: Hydrogen Bond Network among the Functional Groups of Penicillin G and Side Chains of the Conserved Residues in the Active Site

Yasuyuki Fujii,*,† Noriaki Okimoto,‡ Masayuki Hata,† Tetsu Narumi,§ Kenji Yasuoka,|| Ryutaro Susukita,‡ Atsushi Suenaga,§ Noriyuki Futatsugi,§ Takahiro Koishi,‡ Hideaki Furusawa,‡ Atsushi Kawai,‡ Toshikazu Ebisuzaki,‡ Saburo Neya,† and Tyuji Hoshino†

Department of Physical Chemistry, Graduate School of Pharmaceutical Sciences, Chiba University, 1-33 Yayoi-cho, Inage-ku, Chiba 263-8522, Japan, Computational Science Division, The Institute of Physical and Chemical Research (RIKEN), 2-1 Hirosawa, Wako-shi, Saitama, 351-0198, Japan, Genomic Sciences Center (GSC), Bioinfomatics Group, The Institute of Physical and Chemical Research (RIKEN), 1-7-22 Suehiro-cho, Turumi-ku, Yokohama-shi, Kanagawa, 230-0045, Japan, and Department of Mechanical Engineering, Keio University, 3-14-1 Hiyoshi, Kouhoku-ku, Yokohama-shi, Kanagawa, 223-8522, Japan

Received: March 3, 2003; In Final Form: June 23, 2003

Molecular dynamics simulation was performed on class A β-lactamase binding penicillin G (pen G). The structure of the acyl enzyme intermediate (AEI) was derived from the crystallographic data of the clavulanic acid bound enzyme. To execute the simulation precisely, the AEI was solvated by nearly 8000 water molecules and the no-cutoff (NCO) method was applied to the calculation of the Coulomb term. The Coulomb term calculation was accelerated with MDGRAPE-2 hardware. In the first step of this study, the relability of the NCO method was confirmed by comparing experimental and computational *B*-factors. We confirmed that the NCO method is much more reliable than the particle mesh Ewald and generalized Born methods. Hence the NCO method was applied for the simulation on AEI. The integrated simulation time was 1.2 ns. It was found from the simulation that Ser130, Asn132, Ser235, Gly237, and Arg244 cooperatively restricted the mobility of pen G moiety by making salt bridges among the side chains of these residues and the C3-carboxyl or C6-amide group of the substrate. The oxyanion hole composed of N atom in the main chain of Ser70 and Gly237 was properly reproduced under aqueous condition. The simulation also shows that it is impossible for Glu166 to act as a general base in the acylation of pen G because the average distance between Glu166 carboxyl oxygens and Ser70Oγ is too far for direct proton transfer (5.2 and 5.5 Å, respectively) and there is no water molecule between Glu166 carboxylate and Ser70Oγ. Molecular dynamics simulation on the substrate free enzyme (SFE) was also carried out and compared with AEI. While no drastic change due to the substrate binding was observed in both the secondary structure and the positions of catalytic residues of the enzyme, the mobility of the catalytic water molecule was strongly restricted by the presence of the substrate.

1. Introduction

Most pathogenic bacteria produce β-lactamases that inactivate the antibiotic efficiency of β-lactam compound. On the basis of the primary structure of proteins, β-lactamases are classified into four major types: class A, B, C, and D.[1] Class A β-lactamase (CAB) is frequently observed in the clinical scene, compared to other classes of β-lactamases.[2] CAB has a serine residue at the 70th position in the catalytic site (Ser70). Another name for CAB is penicillinase because CAB mainly hydrolyzes the β-lactam ring of penicillin compound. Hence, CAB is expected to have extensive intermolecular interaction with penicillin antibiotics. Catalytic process of CAB involves the acylation of CAB and subsequent deacylation. It should be noted that the short-lived intermediate between them is referred to as the acyl enzyme intermediate (AEI).

The motion of the substrate in AEI is considered to be restricted strongly by amino acid residues around the active site to support the catalytic efficiency of CAB. Typical substrates for CAB such as penicillin G (pen G), ampicillin, and amoxicillin have a carboxyl group at the C3 position of thiazolidine and an amide group at the C6 of the β-lactam ring (Scheme 1). It has been proposed that these functional groups have an ability to make several hydrogen bonds with amino acid residues in CAB. Further, similar to serine proteases, the carbonyl oxygen of β-lactam ring (O8) is considered to be stabilized by the "oxyanion hole" that consists of N atoms in main chains of Ser70 and Gln237.[3] Research on these hydrogen bonds contributes to the development of novel β-lactam antibiotics and CAB inhibitor. In the present study, we executed the molecular dynamics (MD) simulation of the AEI to observe a hydrogen bond network among the functional groups of pen G and amino acid residues in CAB. Three-dimensional structural analysis using X-ray diffraction and NMR can be used for observation of the hydrogen bond network between the enzyme and the binding chemical. However, these experimental methods are rarely applied to the AEI because of the high deacylation activity

* To whom correspondence should be addressed. Telephone: +81-043-290-2927. Fax: +81-043-290-2925. E-mail: yfujii@jbirc.aist.go.jp.
† Chiba University.
‡ Computational Science Division, RIKEN.
§ GSC, RIKEN.
|| Keio University.

10.1021/jp034536t CCC: $25.00
Published on Web 08/23/2003

SCHEME 1: Structures of Typical Substrates for Class A β-Lactamase

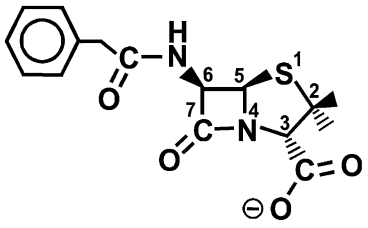

Penicillin G

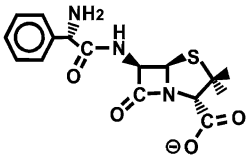

Ampicillin

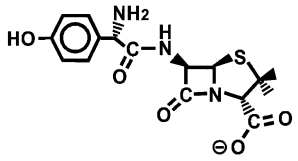

Amoxicillin

of CAB. For this reason, in this study, the structure of the AEI was modeled from an inhibitor−CAB complex using the computational method. (The modeling procedure is described in detail in section 2.1.)

Furthermore, MD on the substrate free enzyme of CAB (SFE) was performed to estimate structural and dynamic differences from those of the AEI. We also focused on the dynamics of a water molecule in the active site. This water molecule is distinct from ordinary solvent water molecules because it is important for the deacylation process. Hence, the catalytic water molecule is sometimes referred to as "deacylating water (D-Wat)". Although Chen et al. suggested that D-Wat in SFE was constrained by side chains of Glu166 and Asn170,[4] the effect of a substrate to bind the D-Wat has never been examined. In this study, the mobility of D-Wat in the presence of the substrate was evaluated by a comparison of dynamic features of the water molecule in the AEI and in the corresponding SFE.

As is well-known, the result of MD simulation mainly depends on the empirical force field parameter set and the calculation method of long-range electrostatic interactions. In principle, the force field parameters define the interactions among the atoms that associate with a covalent bond. In this study, however, we intended to focus on the hydrogen bond network. The hydrogen bond interaction is not a covalent bond. The nature of the hydrogen bond is attributed to the nonbond interaction. Further, the strength of the hydrogen bond is greatly influenced by atomic charges around the hydrogen bond. Therefore, the electrostatic interactions should be very precisely calculated. In most recent MD studies, the particle mesh Ewald (PME) method[5] is utilized for the calculation of long-range electrostatic interactions. The generalized Born (GB) model[6] generates the implicit solvent around a solute and provides a solute−solvent electrostatic polarization term. In contrast to the PME and GB methods, the no-cutoff (NCO) method is not an approximation. However, MD simulation using NCO is only applicable for isolated systems. Hence, none of the three methods has a clear validation for computational reliability. We believe that the polished theory finely reproduces experimental results, and compatibility between experimental and theoretical results is required to confirm the reliability of the theory. MD simulation is mainly executed to explore the dynamic properties of the molecule. The dynamics is attributed to fluctuations of atoms in the molecules. Therefore, to execute a trustworthy MD simulation, we have to select a calculation method that reproduces atomic fluctuation in the molecule. The *B*-factor was used for the evaluation of the trustworthiness because the *B*-factor can be obtained from both experimental and theoretical studies. To examine the reliability of the above three calculation methods, the *B*-factor of SFE from an X-ray diffraction study and the corresponding values obtained from the three simulations using PME, GB, and NCO were compared.

2. Method

2.1. Construction of a Computational Model Representing the Acyl Enzyme Intermediate. In the present study, the AEI was constructed from crystal structural data 1BLC[7] that is stored in the Protein Data Bank (PDB) because the crystal structural data were very suitable for the initial structure of the AEI construction (see the Appendix). The three-dimensional structure of the AEI crystal was determined at 2.2 Å resolution. This AEI model was used for the initial structure of the MD simulation. As for the SFE model, the crystal structure of *Staphylococcus aureus* PC-1 WTE (3BLM) at 2.0 Å resolution was employed.[8] To build the AEI structure from 1BLC, energy minimizations and MD calculation were performed. The united atom force field[9] was applied except for the bound chemicals (clavulanic acid or pen G) and seven amino acid residues that were located at the active site (Ser70, Lys73, Ser130, Asn132, Glu166, Lys234, and Gln237). For the active site residues, an all-atom force field[10] was applied. The solvent used was the TIP3P water model,[11] and about 4000 water molecules were generated by the Monte Carlo method. The box size is 67.5 Å $\times$ 54.7 Å $\times$ 47.4 Å. The MD simulation was executed starting from the energy-minimized structure. The energy minimization was applied only for solvent initially, followed by the relaxation of the whole system. In the energy minimization on the whole system, the steepest descent method was used in the early calculation cycle and then the conjugate gradient method was employed later. The temperature of the whole system was gradually increased by heating from 5 to 300 K for the first 20 ps; then it was kept at 300 K for the next 100 ps simulation. To simplify these calculations, the SHAKE procedure[12] was applied to constrain all covalent bonds involving H atoms. The time step was 1.0 fs. The Coulomb term and van der Waals interaction were truncated at 8 Å.

Since the β-lactam ring and the adjacent five-membered ring of clavulanic acid had been cloven in the original PDB data, the inhibitor was restructured by closing the two rings. Then the initial structure was constructed by superimposing the β-lactam ring of pen G on that of clavulanic acid. The fluctuation of the location of each atom was considerably less under an aqueous condition in the MD calculation of 100 ps at 300 K, and the changes in the distance of every hydrogen bond (we regarded a noncovalent bond below 3 Å as a hydrogen bond) were not more than 0.1 Å during the 100 ps. The minimization and MD simulation were performed with the program Amber, version 6.[13] The atomic charges in clavulanate linked or pen G bound Ser70 were derived from the electrostatic potential that was determined by B3LYP/ 6-31G(d,p) calculation.[14]

2.2. Molecular Dynamics Simulation Process To Obtain the System Equilibrated. The model of constructed AEI was spherically solvated by about 8000 water molecules and an all-atom force field[10] was applied to all residues and solvent molecules. To remove the structural tension, energy minimization was performed. The minimization protocol was similar to that of the AEI modeling. In the heating procedure, the temperature of the whole system was gradually raised from 5 to 300 K for 60 ps. Finally 1.2 ns MD simulation was performed starting from the last atomic configuration of the heating

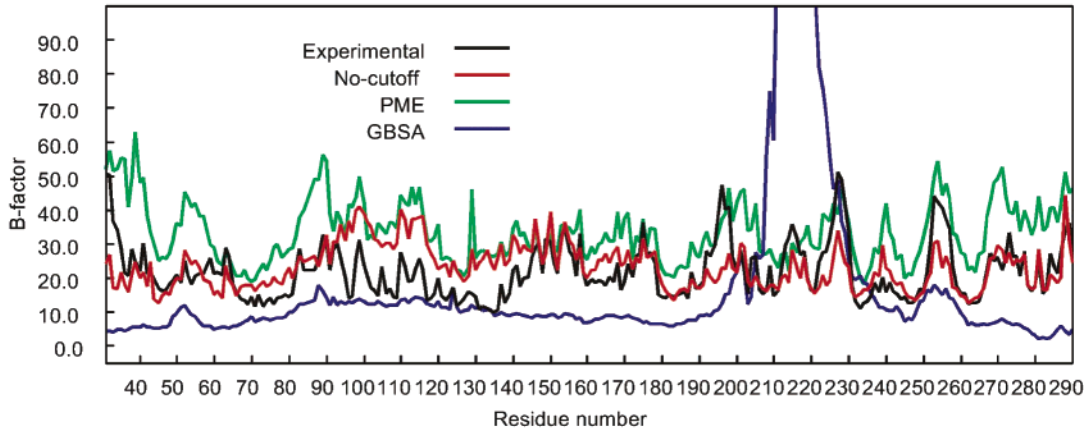

Figure 1. Residue averages of *B*-factors derived from crystallographic data and MD simulations based on several calculation methods.

procedure. The boundary potential was applied to keep the water sphere and volume of the system. Hence this simulation was under NVT conditions. The force constant of the boundary potential was 1.5 kcal/mol/ Å. Similar to the AEI modeling procedure, the SHAKE method[12] was applied to constrain bond lengths involving H atoms and the time step was 1.0 fs. The Coulomb interaction and van der Waals term were explicitly calculated without any approximation by using MDGRAPE-2.[15] The trajectories at the temperature (300 K for 1.2 ns) were considered to be the most probable structure under physiological conditions and were analyzed in detail.

2.3. Comparison of Coulomb Term Calculation Methods Using the *B-Factor*. The experimental *B*-factor was taken from the PDB file of the SFE (3BLM).[8] To collect the MD-derived *B*-factors, MD simulations on SFE using three methods (PME, GB, and NCO) were performed. The integrated times of the simulations were 1.2 ns. The convergences of the simulations were confirmed by root-mean-square (rms) deviation. The calculation of MD-derived *B*-factors requires rms atomic fluctuation (eq 1).[16]

$$B = \frac{8}{3}\pi^2\sqrt{(r_j - \langle r_j \rangle)^2} \qquad (1)$$

The fluctuation was obtained from 200 atomic configurations that abstracted from the simulations during 1.1−1.2 ns at 0.5 ps intervals. The methodological details of NCO simulation were similar to that of the simulation on the AEI (section 2.1). The details of MD simulations using PME and GB methods are described in the Appendix. The *B*-factor of each amino acid residue was obtained to simplify the examination. Because the crystallographic data do not contain the *B*-factor of hydrogen atoms, the theoretical residue *B*-factors were calculated by averaging over the *B*-factor of heavy atoms in each amino acid residue.

3. Results

3.1. Advantage of the Noncutoff Method. Comparison of MD-derived *B*-factors with the experimental *B*-factor is shown in Figure 1. The *B*-factors that were obtained from NCO simulation were considerably compatible with those from experiment. To compare NCO with other methods, the similarity score *D* was calculated. The score *D* was defined by eq 2.

$$D = \frac{\sum_i^N \sqrt{(B_{iT} - B_{iE})}}{N} \qquad (2)$$

B_{iE} denotes the experimental *B*-factor of residue *i*. B_{iT} means the MD-derived *B*-factor. *N* is the number of residues in the enzyme (CAB contains 257 residues). Hence the value *D* shows us the reliability of each method. The value of *D* obtained from NCO *B*-factor was only 8.3. The corresponding values from PME and GB were 13.8 and 31.8, respectively. It is well-known that the *B*-factor can have many contributions other than thermal fluctuation. However, it is significant that the *D* between NCO and experiments was the lowest. Further, we can observe from Figure 1 that undulation of the *B*-factor by *N* is partially similar between NCO and experimental data (especially from residues 35 to 60, from 80 to 90, from 145 to 160, and from 200 to 290). From the strong similarity, it is hard to conclude that there is no correspondence between NCO and the experimental data. Hence we consider that this result is almost enough to suggest the reliability of the NCO method. This result also indicated that the molecular fluctuation of CAB is mainly dominated by the isotropic motion. Therefore, in this study, the NCO method was adapted for the simulation on the AEI and the discussion was developed based on the results obtained by the NCO simulation. It should be noted that the PME method might be the second choice because the PME-derived *B*-factor resembles the NCO feature by rescaling the vertical axis in Figure 1.

3.2. Intermolecular Hydrogen Bond Network between the Enzyme and the Substrate pen G. To judge the convergence of the NCO simulation on the AEI and solvent system, the positional root-mean-square (rms) deviation of the obtained MD trajectory was calculated. For the calculation of the deviation, the atomic configuration at the last point of the heating procedure was used as the zero point of deviation. Time evolution of the rms deviation for all atoms in the whole AEI and the main chain atoms is shown in Figure 2. Consequently, we judged that the simulation was converged and the system was equilibrated because the change in the deviation of the whole and also that of the main chain were below 0.1 Å after about 600 ps. The two deviation curves (whole and main chain) became steady at nearly 1.6 and 1.2 Å, respectively. The catalytically and structurally important interatomic distances were observed in the 1.2 ns simulation. The average atomic distances are shown in Figure 3. It has been found that several amino acid residues generate hydrogen bonds with the functional groups of the degraded substrate and contribute to the stability of the substrate. The C3-carboxyl group of pen G has two oxygen atoms (O1 and O2). The distances of O1−Arg244Nη and O1−Ser235Oγ were within an ordinary range of hydrogen bond during the simulation. The averages of the two distances

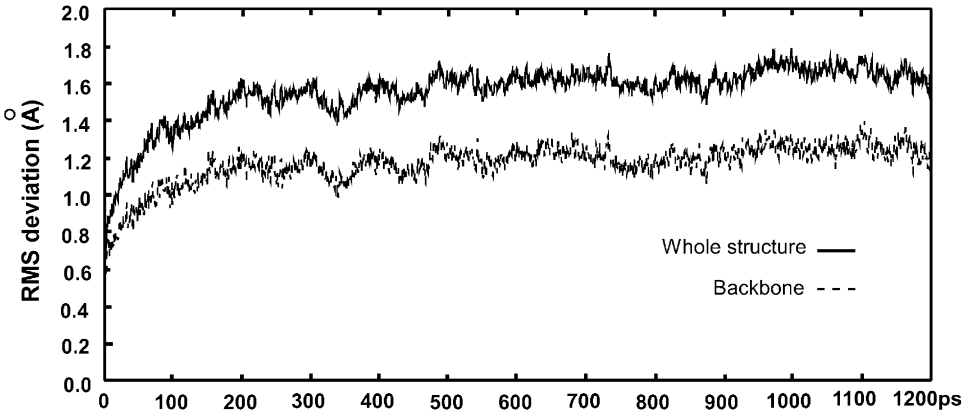

Figure 2. rms deviation of the AEI structure during MD simulation. The rms deviation was calculated with respect to the last structure of the heating stage.

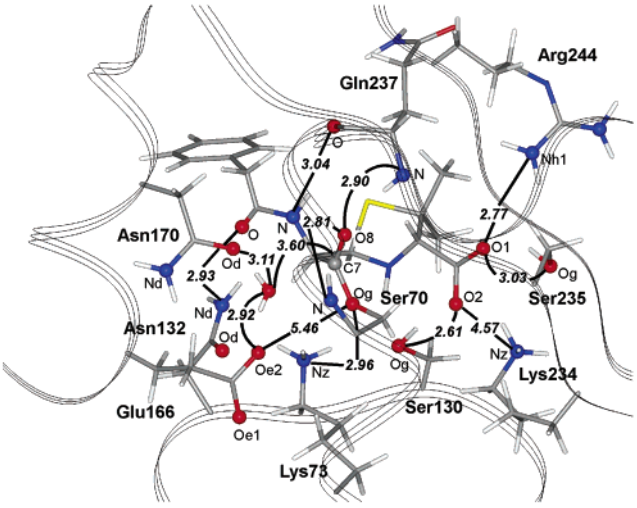

Figure 3. Representation of pen G bound active site in class A β-lactamase. The values indicate average interatomic distance over 1.2 ns.

were about 2.8 and 3.0 Å, respectively. These distances indicate that O1 of the C3-carboxyl group makes two rigid hydrogen bonds with the side chains of Arg244 and Ser235. The average distance between O2 and Ser130Oγ was 2.6 Å. The average distance of O2−Lys234Nζ was 4.6 Å. Accordingly, the C3-carboxyl group strongly interacts with the hydroxyl group of the Ser130 side chain, whereas the interaction between the C3-carboxyl group and the amino group of Lys234 side chain is not preserved. The distance between the carbonyl oxygen of the C6-amide group in pen G and Asn132Nδ appeared to be within the effective range of hydrogen bond during the simulation. The average of the distance was about 2.9 Å. The average distance between the N atom in the C6-amide group and the carboxyl oxygen in the main chain of Gln237 was about 3.0 Å. It was considered from the results that the motion of the C6-amide group is restricted by two hydrogen bonds with the side chain of Asn132 and the main chain carbonyl group of Gln237. The carboxyl oxygen of the degraded β-lactam of pen G (O8) would be trapped by an "oxyanion hole" that consists of two NH groups of the main chains in Ser70 and Gln237. The distances between O8 and Ser70N and O8 and Gln237N were observed within the range of the hydrogen bond in the present study. The average of the two atomic distances was 2.8 and 2.9 Å, respectively. These results indicate that the two hydrogen bonds are fairly rigid, and then O8 is constrained by the oxyanion hole.

TABLE 1: Comparison of Average Interatomic Distances between the AEI and SFE[a]

	interatomic distance[b] (Å)	
	AEI	SFE
Ser70Oγ−Lys73Nζ	2.96	3.25
Ser70Oγ−166Oϵ1	5.18	4.57
Ser70Oγ−166Oϵ2	5.46	5.38
Ser70Oγ−Ser130Oγ	4.24	4.64
Lys73Nζ−Ser130Oγ	5.42	5.27
Lys73Nζ−Asn132Oδ	2.78	2.79
Lys73Nζ−166Oϵ1	2.78	2.86
Ser130Oγ−Lys243Nζ	2.79	3.14

[a] These distances are important for consideration in the catalytic mechanism of CAB. [b] MD average over 1.2 ns.

3.3. Examination of Substrate Binding Effect to the Enzyme-Specific Structure. The substrate binding to an enzyme sometimes causes a drastic conversion of the enzyme structure. In this study, we also examined the substrate binding effect on the structure of CAB. To obtain the SFE structure under physiological conditions, the average structure of SFE was obtained from the trajectory of the NCO simulation and was calculated from 200 atomic configurations that appeared in the simulation from 1.1 to 1.2 ns at 0.5 ps intervals. The average structure of the AEI was obtained in a similar manner. To clarify the change in the whole structure due to the substrate binding, the average structures of SFE and AEI were superimposed by minimizing the positional deviation of these corresponding backbone atoms. The positional rms deviation between the whole structure of SFE and AEI was only 1.1 Å. Hence the SFE structure almost coincided with the AEI. This means that the substrate binding hardly affects the whole structure in the case of CAB. Next, we examined the partial structural conversion due to the substrate binding. Supposing that the most important partial structural conversion would appear at the catalytic site, several distances among six residues in the active site of SFE and the AEI were measured to observe structural changes in the catalytic site of CAB. The distances are shown in Table 1. The measured distances indicate that the active site of SFE is similar to that of the AEI. Consequently, a drastic change was not observed from the structural viewpoint.

3.4. Substrate Binding Effect on the Mobility of the Deacylating Water Molecule. The deacylation of CAB corresponds to the hydrolysis of an ester bond between the degraded substrate and the hydroxyl group of Ser70 in the AEI. In our previous study, quantum chemical (QM) calculations clarified the deacylation mechanism in which a water molecule becomes nucleophilic and attacks the carbonyl carbon of the degraded

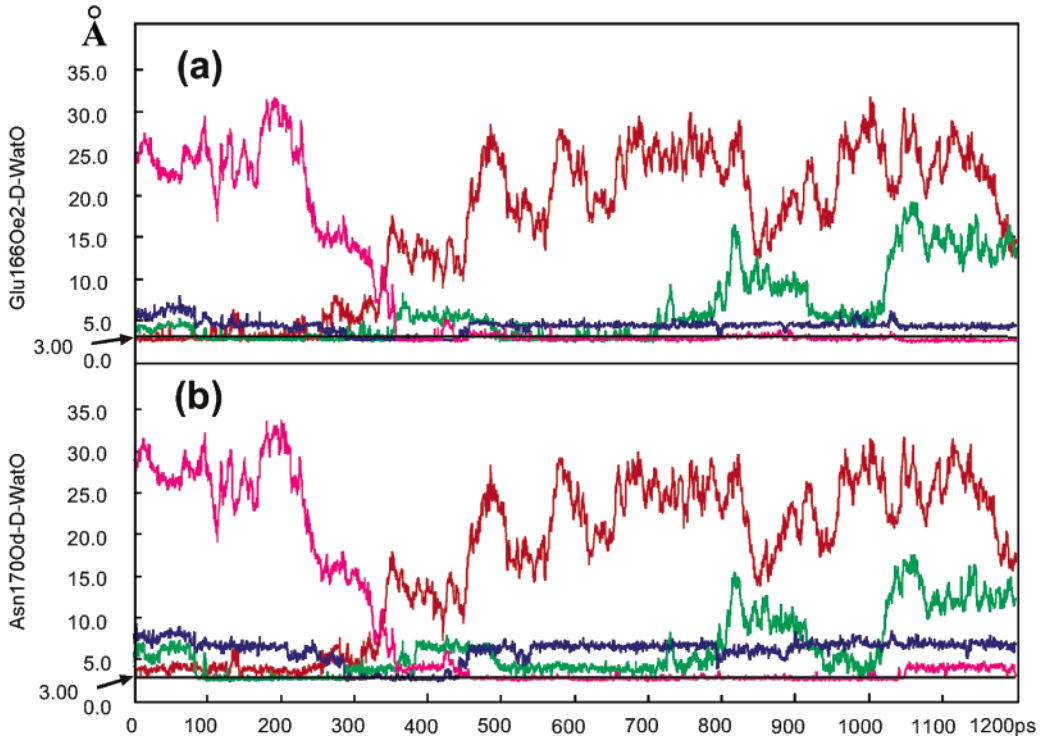

Figure 4. Change in distances from the oxgen of the four water molecules to Glu166Oϵ2 (a) and Asn170Nδ1(b) during MD simulation on the SFE. The ordinate is the distance in angstroms, and the abscissa is the time in picoseconds. The horizontal line through each graph represents the criterion of hydrogen bond distance (3.0 Å).

substrate (C7).[17] Figure 3 informs us that a water molecule is located near C7 in the AEI. This result was very consistent with the previous study. The average interatomic distances between the oxygen in the water molecule (Ow) and two oxygens in Glu166 side chain (O1 and O2) were calculated. The averages of the two distances were 3.1 and 2.9 Å, respectively. Accordingly, the water molecule makes two hydrogen bonds with the carboxyl group of Glu166. In the nucleophilic attack mechanism, the carboxyl group of Glu166 side chain removes an H atom from D-Wat. Therefore, the presence of the hydrogen bonds indicates that the water molecule is D-Wat. Further, the hydrogen bonds between Ow and N atom in the amide group of Asn170 side chain (Asn170Nδ) was observed, and the average of the distance was 3.1 Å (Figure 3). This suggests that the D-Wat in the AEI is held by not only Glu166 and but also Asn170. In the simulation on SFE, a water molecule was held by Glu166 and Asn170. This was similar to the simulation of the AEI. However, we found that the water molecule held in SFE was exchangeable. The time evolutions of distances between the oxygen of the held water molecule and the carboxyl oxygen of Glu166 and the amide group oxygen of Asn170 are shown in parts a and b, respectively, of Figure 4. In the beginning of the simulation, a water molecule was held by Glu166 and Asn170. However, another water molecule entered the active site at about 100 ps and was held by the two residues. This means that the initial water molecule was replaced by the second one. The second water molecule was held by the two residues from ~100 to 300 ps. In the simulation from nearly 300 to 400 ps, the next water molecule was held by the residues alternatively to the previous water molecule. The last water molecule entered between the two residues at nearly 450 ps and was held by the two residues from the entry to the end of the simulation. Accordingly, the exchange of water molecules occurs three times during only 1.2 ns. In contrast to the result of SFE, the held water was stable in the AEI. It should be noted that this is the remarkable difference between SFE and the AEI.

3.5. Catalytically Important Internal Hydrogen Bonds. The distances among the catalytic residues in the average structure of the AEI provide us great implications for the catalytic mechanism of the enzyme. The average distances between Ser70Oγ and two carboxyl oxygens in Glu166 (Oϵ1 and Oϵ2) were nearly 5.2 and 5.5 Å. The average distance of Ser70Oγ from Lys73Nζ was about 3.0 Å. The distance between the carboxyl oxygen in Glu166 side chain and Ser70Oγ was too distant for direct proton migration. Conversely, the distance of Ser70Oγ−Lys73Nζ indicates that a proton of Lys73 can transfer to Ser70Oγ. Figure 5a shows the time development of the distances between Ser70Oγ and the two carboxyl oxygens in Glu166. The distance between Ser70Oγ and Glu166Oϵ1 suddenly increased at nearly 170 ps. To find a cause for the sudden increase of the distance, the time development of the Glu166Oϵ2−Asn170Nδ distance was measured. The graph of the distance is shown in Figure 5b. It was found from the plot that Glu166Oϵ2 made a new hydrogen bond with Asn170Nδ at nearly 170 ps. The new hydrogen bond was retained rigidly through the rest of the simulation. Therefore, the increase of the distance between Ser70Oγ and the carboxyl group of Glu166 resulted from the generation of this new hydrogen bond between Glu166Oϵ2 and Asn170Nδ.

4. Discussion

4.1. Restriction of the Substrate Mobility by Hydrogen Bond Network. The location of a substrate in an enzyme must be restricted for the catalytic efficiency of the enzyme. Typical substrates for CAB such as pen G usually have a C3-carboxyl and a C6-amide group. As shown in Figure 3, seven hydrogen bonds were detected between the CAB and the two functional groups of the substrate. In this section, we provide several considerations on the substrate binding from the viewpoint of the hydrogen bond network observed in the present study and in the available experimental data.

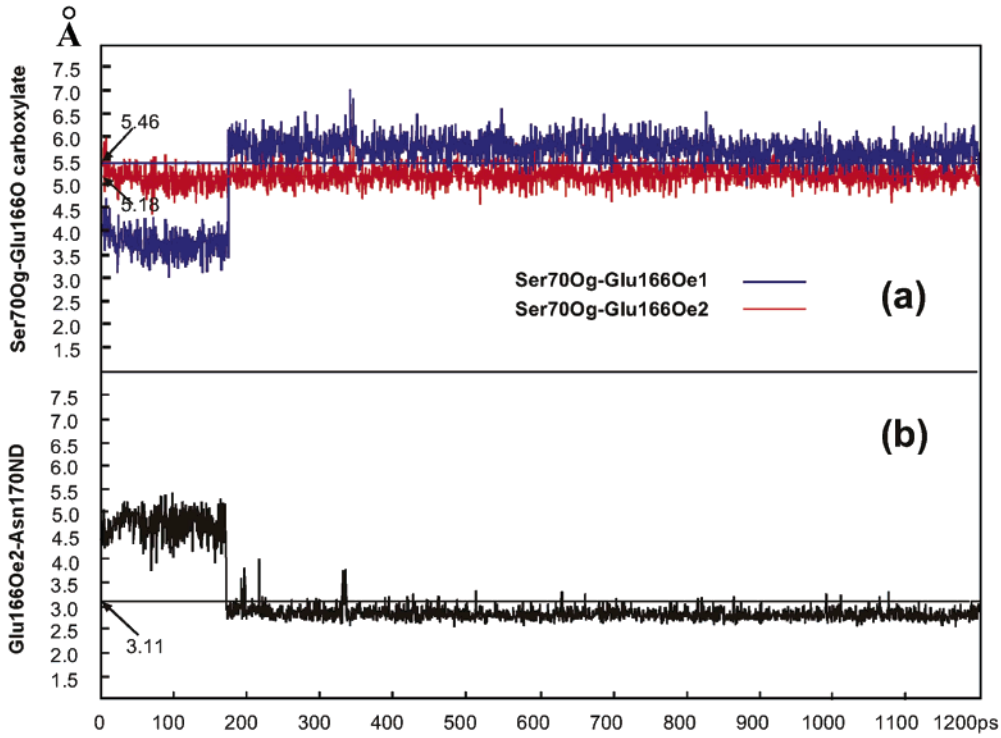

Figure 5. Change in distances from Glu166Oϵ1 and Glu166Oϵ2 to Ser70Oγ (a) and Asn170Nδ (b) during MD simulation on the AEI. The ordinate is the distance in angstroms, and the abscissa is the time in picoseconds. The horizontal line through each graph represents the average distance over the entire simulation.

4.1.1. Hydrogen Bonds Including the C3-Carboxyl Group. pen G derivatives that have a methyl ester[18] or amide group[19] at C3 in the thiazolidine ring were reported to be poor substrates of CAB. Therefore, the C3-carboxyl group is critical for the substrate recognition of CAB. It has been found from the present study that the C3-carboxy group makes three hydrogen bonds with amino acid residues that are located near the active site. One oxygen atom in the C3-carboxyl group makes hydrogen bonds with the hydroxyl group of Ser235 and the guanidium group of Arg244. Another oxygen atom interacts with the hydroxyl group of Ser130. Therefore, the mobility of the C3-carboxyl group is restricted by Ser130, Ser235, and Arg244. In the three amino acid residues, however, the conserved residue in CAB is only Ser130. A couple of experimental works has shown that the mutant Ser130Ala has less affinity to the substrate.[20] This result of the mutation study is consistent with our study. The amino acid residue at the 235th position in CAB is serine or threonine.[2] Similarly to serine residue, threonine has a hydroxyl group in its side chain. Hence, it is safe to consider that Thr235 makes a hydrogen bond with C3-carboxyl oxygen. Arg244 is not the conserved residue.

In the CABs induced from plasmids of TEM30 and TEM31, the amino acid residues at the 244th position are serine and cysteine, respectively.[21] Although serine and cysteine have a polar group in their side chains, the side chain lengths of these residues are obviously shorter than that of arginine. Therefore, the restriction of mobility of the C3-carboxyl group that was observed in this study must be impossible in the CABs produced from TEM30 and TEM31. Imtiaz et al. reported that an artificial mutation at the 244th position causes a decrease of affinity to the substrate.[22] Further, the catalytic activity of this mutant was also lower compared with WTE. Hence the mobility restriction of the C3-carboxyl group correlates with the catalytic efficiency of CAB. In our previous study, it was clarified that the C3-carboxyl group took part in the catalytic reaction of CAB.[17] Therefore, the result of the mutation study is in accord with our results.

As described in section 2.1, the AEI structure used was modeled from the crystal structure of an acyl enzyme that consists of clavulanic acid and CAB. It was found from the structural data[7] that a water molecule made a bridge between the guanidium group in Arg244 and the C3-carboxyl group. In this study, however, the water molecule was not detected in the average AEI structure. The water molecular was excluded from the space between Arg244 and the C3-carboxyl group in the modeling procedure of the AEI structure. At the end of the modeling procedure, the guanidium group in Arg244 directly interacted with the C3-carboxyl group. The appearance of the water molecule in the crystal structure of clavulanate−CAB complex might result from the collapse of the five-membered ring of clavulanate. It has been frequently reported that the C3-carboxyl group also interacted with the amino group of Lys234.[2] The residue Lys234 is entirely conserved in CAB.[21] In the crystalline form of clavulanate complex, the distance between the N atom of the amino group of Lys234 (Lys234Nζ) and one of the C3-carboxyl oxygens was found to be 2.33 Å. Although the distance is too small for a hydrogen bond, this observation indicated that the amino group of Lys234 was located near the C3-carboxyl group. In the present study, however, the hydrogen bond between Lys234Nζ and the C3-carboxyl group was dissolved during the heating procedure of the simulation. In the last point of the heating procedure, Lys234Nζ made a hydrogen bond with Ser130Oγ. The average distance between Lys234Nζ and Ser130Oγ was 2.73 Å. This suggests that the amino group of Lys234 restricts the orientation of the hydroxyl group of Ser130 to form the hydrogen bond between Ser130Oγ and the C3-carboxyl oxygen. In other words, Lys234 binds the substrate to the active site via the hydroxyl group of Ser130.

4.1.2. Hydrogen Bonds Including the C6-Amide Group. Two interactions between the C6-amide side chain of the substrate

SCHEME 2: Hypothetical Mechanisms of TI Formation in the Acylation Step[a]

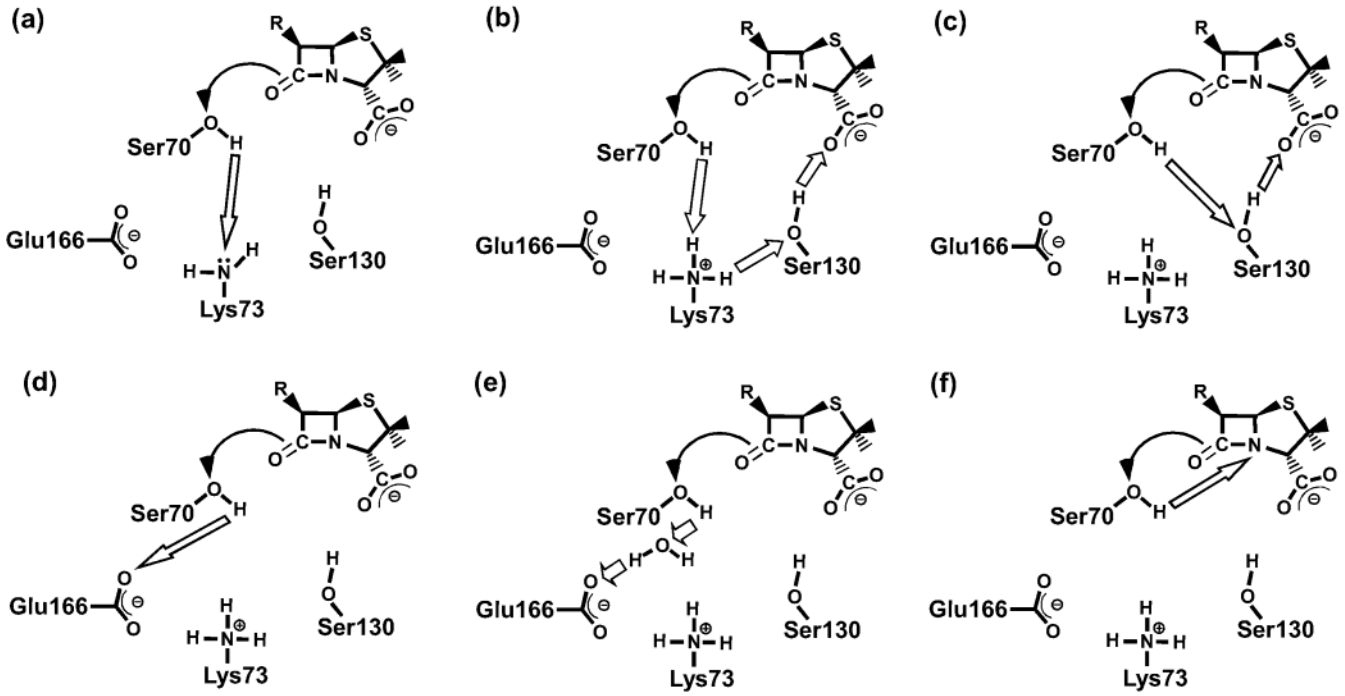

[a] Each mechanism has been proposed in earlier work (see text). Arrows indicate atomic migration.

and polar groups in the catalytic residues were observed in section 3.2. The carbonyl oxygen and the amide group of the C6 side chain made hydrogen bonds with the amino group of Asn132 side chain and the carbonyl oxygen in the main chain of Gln237, respectively. Asn132 is known to be highly conserved in CAB.[2] It was proposed that the role of Asn132 was only to take part in the substrate binding.[23] This opinion does not conflict with our result. However, it was reported that the point mutation at the 132nd position leads to a decline of catalytic efficiency of the enzyme.[24] How does the amide group of Asn132 concern the catalytic process? To answer the question, we calculated the average distance between the carbonyl oxygen of Asn132 side chain and Lys73Nζ because Lys73 is essential to the catalytic mechanism of CAB[25] and Lys73 is the nearest catalytic residue from Asn132. The average distance was within hydrogen bond range (3.0 Å). Lys73 is considered to be fairly stable, despite the long reach of its side chain, so it can participate in the catalytic mechanism. Judging from our result, the stability of the amino group of Lys73 would result from the formation of the internal hydrogen bond. Therefore, we can speculate that Asn132 indirectly contributes to the catalysis of CAB by the restriction of the functional amino group of Lys73. In contrast to Asn132, Gln237 is not conserved in CAB.[21] We consider that the variation of amino acid residue at the 237th position has little influence on the hydrogen bond with the amino group in the C6 side chain because the hydrogen bond consists of the main chain of residue 237. In the clinical scene, clavulanic acid and sulbactum are usually used for inhibition of the enzymatic activity of CAB. These inhibitors are devoid of the C6 side chain. These inhibitors binding to Ser70 rarely leave the active site. This means that the deacylation reaction is hard to occur after the acylation of CAB by these inhibitors. In the acyl enzyme that consists of the inhibitor moiety and CAB, the location of the moiety might be unstable relative to the typical substrates because of the absence of the hydrogen bond between C6 side chain and Asn132 or Gln237. Since the high mobility of the moiety is considered to disturb the deacylation reaction, the inactivation of CAB by these inhibitors might arise from the absence of C6 functional group.

4.1.3. Carbonyl Oxygen of the Substrate Trapped in Oxyanion Hole. It is well-known that serine hydroxylases such as trypsin and acetylcolinesterase generally have the substrate trapping system that is referred to as "oxyanion hole". Pratt et al. suggested that CAB also has an oxyanion hole in the catalytic site.[3b] Several crystal structures of the AEI analogues demonstrated that the carbonyl oxygen of penicillins or substrate-imitating inhibitors was held by the oxyanion hole.[7,8,23,26−28] The oxyanion hole in CAB consists of two amide groups in the main chains of Ser70 and Gln237. As described in section 2.1, the AEI model used in this study was constructed from the crystal analysis data of the AEI analogue that consists of clavulanate and CAB. Similarly to other AEI analogues, the structural data of the AEI analogue indicated that the carbonyl oxygen of the clavulanate moiety made two hydrogen bonds with the main chain of Ser70 and Gln237.[7] It was found that the two hydrogen bonds were completely retained in the whole of the MD simulation on the constructed AEI. The deviations of the distances between N atoms of the main chains of Ser70 and Gln237 and the carbonyl oxygen of the substrate during the simulation were 0.09 and 0.12 Å, respectively. These deviations of the hydrogen bond distance were the first and second smallest in the corresponding values of all hydrogen bonds between the substrate and the enzyme. Accordingly, the oxyanion hole provides the very rigid substrate restriction in the AEI. It should be noted that the oxyanion hole not only contributes to the restriction of the mobility of the substrate but also facilitates the hydrolysis of the substrate by inducing the electronic polarization of the carbonyl group.[29]

4.2. Characterization of the Substrate by the C6 Side Chain. Although the substrate binding effect on the enzymatic structure would be one of the issues of interest in enzymonology,[30] no drastic structural difference between the structures of SFE and the AEI was observed. This means that pen G is very suitable for the catalytic cite of CAB and hardly affects the

structure of CAB. The affinity of pen G to CAB is considerably higher than those of other β-lactam compounds.[31] We found that the position of D-WAT in SFE is considerably unstable relative to that in the AEI. Judging from this finding, it can be concluded that pen G binding facilitates the catalysis of CAB due to the stability of a D-WAT rather than the change of the enzymatic structure. Figure 3 shows that the C6 side chain of pen G is located covering over the catalytic D-WAT. The good substrates for CAB such as pen G have a huge side chain at C6. The side chain of these substrates is usually a hydrophobic group. Hence, we speculate that the hydrophobic side chain in these substrates isolates the D-WAT from bulk solvent waters around the enzyme and stabilizes the location of the D-WAT in the active site. As described in section 4.1, CAB inhibitors such as clavulanic acid and sulbactum have no C6 side chain; therefore, we suggested that the pharmacological effect of these inhibitors is caused by the high mobility of these moieties in AEI. In addition to that suggestion, the effect of inhibitors could arise from the instability of the D-WAT by the absence of the hydrophobic group at C6. Maveyraud et al. found that 6α-hydroxymethylpenicillic acid (6APA) also inactivates the catalytic ability of CAB.[27] Imipenems also have 6α side chains and inhibit CAB catalysis. It was reported that the location of D-WAT in the active site was disorderd by the 6α side chain.[28,32] We have demonstrated that the D-WAT is held by the side chains of Glu166 and Asn170 in the MD simulation on the AEI. The C6 side chain of the substrate is oriented toward the direction opposite that of the side chain of these inhibitors. The direction is referred to as the "β-side". In our MD, the 6β side chain of the substrate never disturbed the position of D-WAT. Therefore, it is concluded that the 6β-functional group in a β-lactam compound stabilizes the D-WAT at a position adequate to facilitate the deacylation catalysis in cooperation with Glu166 and Asn170 and that the good substrate for CAB is characterized by the 6β side chain. To investigate the motion of the D-WAT in the acyl enzyme complexes that consist of these inhibitors, we now perform further simulations.

4.3. Tetrahedral Intermediate (TI) Formation Mechanism in the Acylation Step of the CAB Catalysis. Numerous experimental and theoretical studies have been performed to clarify the acylation mechanism of CAB. Most of these studies presented a consensus that the TI formation was caused by a nucleophilic attack on the C7 by Ser70Oγ in concert with a proton abstraction from the hydroxyl group of Ser70.[33] However, the proton abstraction mechanism was unclear. Several mechanisms proposed on the TI formation are depicted in Scheme 2. In these sub-sequences, we attempt to evaluate these hypothetical mechanisms using the structure of the AEI obtained by the MD simulation. Strynadka et al. have proposed that Lys73 abstracted a proton from Ser70 (a in Scheme 2).[23] Several experimental and theoretical works supported this mechanism.[29,33] The average distance of Ser70Oγ−Lys73Nζ in the AEI in Figure 3 indicates that a proton transfer from Ser70Oγ to Lys73Nζ is fairly possible. However, Damblon et al. revealed by NMR titration study that the pK_a value of Lys73 in SFE was >10.[35] Moreover, Lamotte-Brasseur et al. clarified that the pK_a of this residue in Henri−Michaelis (HM) complex was also >10.[36] These results from the pK_a measurements indicated that the Lys73 was protonated in SFE and the AEI, which was inconsistent with mechanism a. Hence we have to abandon mechanism a by means of the pK_a measurement studies despite the fact that we could give a justification to the mechanism.

Ishiguro et al. proposed a unique mechanism in which a substrate assisted the reaction (b).[37] This hypothetical mechanism involves two elementary reactions. First, the Lys73 in HM complex is deprotonated by C3-carboxyl group of the substrate via the hydroxyl group in Ser130 side chain. Second, the deprotonated Lys73 abstracts a proton from Ser70. The first elementary reaction in this mechanism is a concerted double proton transfer. Although the average distance between C3-carboxyl oxygen and Ser130Oγ was within hydrogen bond range, the average distance of Lys73Nζ−Ser130Oγ was beyond the hydrogen bonding distance (see Table 1). However, the concerted double proton transfer is not completely denied because the long side chain of Lys73 might have a high flexibility to approach Ser130Oγ. Therefore, this mechanism should not be rejected.

Recently, another substrate-assisted mechanism was proposed by Díaz et al. (c).[38] In this mechanism, C3-carboxyl oxygen abstracts a proton from Ser70 via a hydroxyl group in the Ser130 side chain. Our results do not support this mechanism because the average distance of Ser70Oγ−Ser130Oγ is not within the hydrogen bond range in both SFE and the AEI. Moreover, Ser70 and Ser130 do not have enough flexibility, in contrast to Lys73.

Gibson et al. suggested that Glu166 acted as the proton abstractor (d).[39] After the suggestion, a couple of investigations which supported this mechanism were reported.[40] However, our MD simulation indicates that Glu166 is too far for the proton abstraction from Ser70. Therefore, we judge that the mechanism might be impossible.

Lamotte-Brasseur et al. suggested a mechanism that Glu166 abstracts a proton from Ser70Oγ via a water molecule (e).[41] This mechanism has been supported by several studies[42] and a review article.[33] However, in our MD simulation, we could not observe a stable water molecule between Ser70 and the carboxyl group of Glu166 side chain. Moreover, we also could not observe such a situation during the MD on SFE that Ser70 hydroxyl proton was orientated to the carboxyl group of Glu166. Hence the reliability of this mechanism is ambiguous.

The orientation of the hydroxyl proton of Ser70 is in accord with mechanism f, which was proposed by Adachi et al..[43] Further, in the average structure of AEI, the hydrogen atom of N4 in the thiazolidine ring of the substrate seemed to be oriented to Ser70Oγ. Pitarch et al. theoretically revealed that N4 abstracts a proton from a water molecule without any assist in the hydrolysis of penicillin compound under neutral condition, and the stability of N4-protonated form of the substrate was also proved.[44] This result directly suggests that N4 can act as general base catalyst. Therefore, we can agree with this mechanism. Consequently, we conclude from the MD simulations that the two mechanisms b and f are probable. However, we cannot determine the most favorable one between them. Molecular orbital calculations will be effective to determine the reaction mechanism and confirm the possibility of the two mechanisms.

5. Conclusion

MD simulation on the AEI was performed to reveal the hydrogen bond network between the substrate pen G and CAB. We have found from the simulation that Ser130, Ser235, and Arg244 make hydrogen bonds with the C3-carboxylate of pen G. Asn132 and Gln237 form hydrogen bonds with the C6-amide side chain of pen G. It has been observed that the carbonyl oxygen of pen G is held by the oxyanion hole composed of Ser70 and Gln237. Further, the substrate binding stabilizes the deacylation water molecule at a position adequate to facilitate the catalysis. We have also found that the NCO calculation is the best method that properly reproduces the atomic fluctuation derived from the experimental data.

Acknowledgment. The authors thank the Computer Center for the Institute of Molecular Science, for the use of Fujitsu VPP500 computer. The computations were also carried out by the DRIA System at the Graduate School of Pharmaceutical Sciences, Chiba University.

Appendix

How To Select the AEI Analogue as the Initial Structure. As described in section 1, experimental studies cannot approach the structure of the AEI. Instead, a half-dozen of the crystal structures of AEI analogues have been presented in the Protein Data Bank (PDB). To build the AEI structure, we selected an AEI analogue from the candidates. The AEI analogues can be categorized in two groups from the type of the enzyme and the chemicals binding to the enzyme. In one category, the AEI analogues composed the mutant of CAB that loses catalytic ability and a typical substrate of the enzyme. Usually, Glu166 mutant has low deacylation activity. Strynadka et al. have determined the crystal structure of the AEI analogue composed by the Glu166Asn mutant and penG (PDB code 1FQG).[23] This was the first report on AEI analogue structure. The crystal structures of Glu166Asn:Asn170Gln double mutant with pen G (1GHP) or cephaloridine (1GHM) were reported by Chen et al., who revealed that the deacylation activity of CAB depends on not only Glu166 but also Asn170.[26] However, these AEI analogues were not suitable for AEI modeling because the conformation of the carboxyl group of Glu166 side chain was unclear. In another category, the AEI analogues are constructed by a wild-type enzyme (WTE) of CAB and a β-lactam type inhibitor. Mourey et al. reported the crystal structures of NMC-A WTE with 6α-hydroxymethylpenicillanate (1TEM)[27] and 6α-hydroxyethylpenicillanate (1BUL).[28] However, these AEI analogues are also unsuitable for the AEI modeling because the position of D-Wat seemed to be displaced by the 6α side chain of the inhibitors. Although a crystal structure of WTE with imipenem acyl enzyme was determined by Maveyraud et al., the imipenem also has an α-hydroxyethyl side chain at the C6 position.[32] Chen et al. reported another AEI analogue that was composed by WTE from *Staphylococcus aureus* PC-1 with clavulanic acid moiety (1BLC).[7] In this AEI analogue structure, the conformation of Glu166 is clear and the position of the D-Wat is considered to be fairly reliable because the WTE has Glu166 and the clavulanic acid has no 6α side chain. From the considerations, we concluded that the 1BLC is the most suitable structure for the AEI modeling procedure.

Methodological Details of PME and GB Simulation. The PME method is utilized under the periodic boundary condition. The size of the periodic box was 78.7 Å $\times$ 62.2 Å $\times$ 75.9 Å, and nearly 8000 TIP3P water molecules were included in it. In the initial structure, the minimum distance between the protein surface and the boundary was about 9.32 Å. The MD procedure to equilibrate the system was carried out with NPT ensemble, and the desired pressure and density were 1.0 atm and 1.0 g/cm^3, respectively. Fifteen Cl^- counterions were added to the protein to electronically neutralize the system because the PME method is only applicable to the neutral system. The grid spacing was approximately 1.0 Å. The Coulomb and van der Waals terms obtained from the direct calculation were truncated at 15 Å on atom bases. The Coulomb pair list was updated every 0.1 ps.

The GB/SA (generalized Born/solvent-accessible surface area) method was applied for GB calculation in the present study. The Born radii α_i were derived from the pairwise descreening approximation (PDA).[45] The intrinsic radii were calculated using parameters determined by Tsui et al.[46] The value of b_{offset} was -0.9 Å. The dielectric constant ϵ was 78.3.

References and Notes

(1) Abraham, E. P.; Chain, E. B. *Nature (London)* **1940**, *146*, 837.
(2) Matagne, A.; Frère, J.-M. *Biochim. Biophys. Acta* **1995**, *1246*, 109−127.
(3) (a) Herzberg, O. *J. Mol. Biol.* **1991**, *217*, 701−719. (b) Murphy, B. P.; Pratt, R. F. *Biochem. J.* **1998**, *256*, 669−672.
(4) Chen, C. C.; Herzberg. O. *Protein Eng.* **1999**, *12*, 573−579.
(5) Darden, T.; Darrin, Y.; Pedersen, L. *J. Chem. Phys.* **1993**, *98*, 10089−100924.
(6) Still, W. C.; Tempczyk, A.; Hawley, R. C.; Hendrickson, T. *J. Am. Chem. Soc.* **1990**, *112*, 6127−6129.
(7) Chen, C. C. H.; Herzberg, O. *J. Mol. Biol.* **1992**, *224*, 1103−1113.
(8) Herzberg, O. *J. Mol. Biol.* **1991**, *217*, 701−719.
(9) Weiner, S. J.; Kollman, P. A.; Case, D. A.; Singh, U. C.; Ghio, C.; Alagona, G.; Profeta, S., Jr.; Weiner, P. J. *J. Am. Chem. Soc.* **1991**, *106*, 765−784.
(10) Weiner, S. J.; Kollman, P. A.; Nguyen, D. T.; Case, D. A. *J. Comput. Chem.* **1986**, *7*, 230−252.
(11) Jorgensen, W. L.; Chandrasekhar, J.; Madura, J. D. *J. Chem. Phys.* **1983**, *79*, 926−935.
(12) Ryckaert, J. P.; Ciccotti, G.; Berendsen, H. J. C. *J. Comput. Phys.* **1977**, *23*, 327−341.
(13) Case, D. A.; Pearlman, D. A.; Caldwell, J. W.; Cheatham III, T. E.; Ross, W. S.; Simmerling, C.; Darden, T.; Merz, K. M.; Stanton, R. V.; Cheng, A.; Vincent, J. J.; Crowley, M.; Tsui, V.; Radmer, R.; Duan, Y.; Pitera, J.; Massova, I.; Seibel, G. L.; Singh, U. C.; Weiner, P.; Kollman, P. A. *Amber*, version 6; University of California: San Francisco, CA, 1999.
(14) (a) Becke, A. D. *J. Chem. Phys.* **1993**, *98*, 5648−5652. (b) Lee, C.; Yang, W.; Parr, R. G. *Phys. Rev. B* **1998**, *37*, 785−789.
(15) (a) Narumi, T.; Susukita, R.; Ebisuzaki, T.; McNiven, G.; Elmegreen, B. *Mol. Simul.* **1991**, *21*, 401. (b) Narumi, T.; Susukita, R.; Koishi, T.; Yasuoka, K.; Furusawa, H.; Kawai, A.; Ebisuzaki, T. *Proceeding of SC2000*, Dallas, 2000. (c) Narumi, T.; Kawai, A.; Koishi, T. *Proceeding of SC2001*, Denver, 2001.
(16) Brooks III, C. L.; Karplus, M.; Pettitt, B. M. *Proteins*; Wiley & Sons: New York, 1998.
(17) Fujii, Y.; Hata, M.; Hoshino, T.; Tsuda, M. *J. Phys. Chem. B* **2002**, *106*, 9687−9695.
(18) Laws, A. P.; Page, M. I. *J. Chem. Soc., Perkin Trans. 2* **1989**, 1577−1581.
(19) Varetto, L.; De Meester, F.; Monnaie, D.; Marchand-Brynaert, J.; Dive, G.; Jacob, F.; Frère, J.-M. *Biochem. J.* **1991**, *278*, 801−807.
(20) (a) Jacob, F.; Joris, B.; Lepage, S.; Dusart, J.; Frère, J.-P. *Biochem. J.* **1990**, *271*, 399−406. (b) Juteau, J.-M.; Billings, E.; Knox, J. R.; Levesque, R. C. *Protein Eng.* **1992**, *5*, 693−701.
(21) Knox, J. R. *Antimicrob. Agents Chemother*. **1995**, *39*, 2593−2601.
(22) Imtiaz, U.; Billings, E.; Knox, J. R.; Manavathu, E. K.; Lerner, S. A.; Mobashery, S. *J. Am. Chem. Soc.* **1993**, *115*, 4435−4442.
(23) Strynadka, N. C. J.; Adachi, H.; Jensen, S. E.; Johns, K.; Sielecki, A.; Betzel, C.; Suto, K.; James, M. N. G. *Nature (London)* **1992**, *359*, 700−705.
(24) Jacob, F.; Joris, B.; Dideberg, O.; Dusart, J.; Ghuysen, J.-M.; Frère, J.-M. *Protein Eng.* **1990**, *4*, 79−86.
(25) Lietz, E. J.; Truher, H.; Kahn, D.; Hokenson, M. J.; Fink, A. L. *Biochemistry* **2001**, *39*, 4971−4981.
(26) Chen, C. C. H.; Hertzberg, O. *Biochemistry* **2001**, *40*, 2531−2538.
(27) Maveyraud, L.; Massova, I.; Birck, C.; Miyashita, K.; Samama, J.-P.; Mobashery, S. *J. Am. Chem. Soc.* **1996**, *118*, 7435−7440.
(28) Mourey, L.; Miyashita, K.; Swarén, P.; Bulychev, A.; Samama, J.-P.; Mobashery, S. *J. Am. Chem. Soc.* **1998**, *120*, 9382−9383.
(29) Wladkowski, B. D.; Chenoweth, S. A.; Sanders, J. N.; Krauss, M.; Stevens, W. J. *J. Am. Chem. Soc.* **1997**, *119*, 6423−6431.
(30) Mori, K.; Hata, M.; Neya, S.; Hoshino, T.; *Chem-Bio Inf. J.* **2002**, *2*, 147−155.
(31) Juteau, J.-M.; Billings, E.; Knox, J. R.; Levesque, R.-C. *Protein Eng.* **1992**, *7*, 693−9701.
(32) Maveyraud, L.; Mourey, L.; Kotra, L. P.; Pedelacq, J.-D.; Guillet, V.; Mobashery, S.; Samama, J.-P. *J. Am. Chem. Soc.* **1998**, *120*, 9748−9752.
(33) Matagne, A.; Lamotte-Brasseur, J.; Frère, J.-M. *Biochem. J.* **1998**, *330*, 581−598.
(34) (a) Herzberg, O.; Moult, J. *Science* **1987**, *236*, 694−701. (b) Knox, J. R.; Moews, P. C. *J. Mol. Biol.* **1991**, *220*, 435−455.
(35) Damblon, C.; Raquet, X.; Lian, L.-Y.; Lamotte-Brasseur, J.; Fonze, E.; Charlier, P.; Roberts, G. C. K.; Frère, J.-M. *Proc. Natl. Acad. Sci. U.S.A.* **1996**, *93*, 1747−1752.

(36) Lamotte-Brasseur, J.; Lounnas, V.; Raquet, X.; Wade, R. C. *Protein Sci*. **1999**, *8*, 404−409.

(37) Ishiguro, M.; Imajo, S. *J. Med. Chem*. **1996**, *39*, 2207−2218.

(38) Díaz, N.; Suárez, D.; Sordo, T. L.; Mertz, K. M., Jr. *J. Phys. Chem. B* **2001**, *105*, 11302−11313.

(39) Gibson, R. M.; Christensen, H.; Waley, S. G. *Biochem. J*. **1990**, *272*, 613−619.

(40) (a) Knap, A. K.; Pratt, R. F. *Biochem. J*. **1991**, *273*, 85−91. (b) Vijayakumar, S.; Ravishanker, G.; Pratt, R. F.; Beveridge, D. L. *J. Am. Chem. Soc*. **1995**, *117*, 1722−1730.

(41) Lamotte-Brasseur, J.; Dive, G.; Dideberg, O.; Charlier, P.; Frère, J.-M.; Ghuysen, J.-M. *Biochem. J*. **1991**, *279*, 213−221.

(42) (a) Escobar, W. A.; Tan, A. K.; Lewis, E. R.; Fink, A. L. *Biochem. J*. **1991**, *273*, 85−91. (b) Swarèn, P.; Maveyraud, L.; Guillet, V.; Masson, J.-M.; Mourey, L.; Samama, J.-P. *Structure* **1995**, *3*, 603−613.

(43) Adachi, H.; Ohta, T.; Matsuzawa, T. *J. Biol. Chem*. **1991**, *266*, 3186−3196.

(44) Pitarch, J.; Ruiz-López, M. F.; Silla, E.; Pascual-Ahuir, J.-L.; Tuñón, I. *J. Am. Chem. Soc*. **1998**, *120*, 2146−2155.

(45) (a) Hawkins, G. D.; Cramer, C. J.; Truhlar, G. D. *Chem. Phys. Lett*. **1995**, *246*, 122−129. (b) Hawkins, G. D.; Cramer, C. J.; Truhlar, G. D. *J. Phys. Chem*. **1996**, *100*, 19824−19839.

(46) Tsui, V.; Case, D. A. *J. Am. Chem. Soc*. **2000**, *122*, 2489−2498.